Magnetotransport in doped polyaniline

2005 J. Phys.: Condens. Matter 17 1947

(http://iopscience.iop.org/0953-8984/17/12/017)

INSTITUTE OF PHYSICS PUBLISHING JOURNAL OF PHYSICS: CONDENSED MATTER

J. Phys.: Condens. Matter **17** (2005) 1947–1960 doi:10.1088/0953-8984/17/12/017

Magnetotransport in doped polyaniline

A K Mukherjee and Reghu Menon

Department of Physics, Indian Institute of Science, Bangalore 560 012, India

Received 10 August 2004, in final form 21 February 2005
Published 11 March 2005
Online at stacks.iop.org/JPhysCM/17/1947

Abstract

Conductivity and magnetotransport studies have been carried out in polyaniline (PANI) doped with 2-acryloamido-2-methyl-1-propane sulfonic acid (AMPSA), camphor sulfonic acid (CSA) and dodecylbenzene sulfonic acid (DBSA). Both PANI-AMPSA and PANI-CSA show a metallic positive temperature coefficient of resistivity above 150 K, and the data down to 1.6 K show that the systems are near the critical regime of metal–insulator (M–I) transition, whereas PANI-DBSA shows hopping transport. The magnetoconductance (MC) in PANI-AMPSA is positive (negative) in transverse (longitudinal) directions. The anisotropic MC in PANI-AMPSA is due to the interplay of contributions from weak localizations, electron–electron interactions and hopping transport. This suggests the presence of local molecular-scale quasi-two dimensional (q-2D) ordered regions in PANI-AMPSA, which are absent in the other two systems. The MC is weakly (strongly) negative in PANI-CSA (PANI-DBSA). The data analysis yields consistent values for various length scales (e.g., inelastic scattering length, localization length, etc) according to this model. These results indicate that the surfactant counterion plays a major role in local molecular-scale ordering and charge transport properties in doped PANI.

1. Introduction

The intrinsic and extrinsic contributions to charge transport in disordered quasi-one-dimensional (q-1D) systems like conducting polymers are still a contentious issue [1, 2]. Among various conducting polymers, the counterion-induced processed polyaniline (PANI) system is an ideal system for investigating the role of morphology in metal–insulator (M–I) transitions [3, 4]. Recently Tzamalis *et al* [5] have reported a detailed transport measurement study in PANI doped by 2-acryloamido-2-methyl-1-propane sulfonic acid (AMPSA) and camphor sulfonic acid (CSA). Prior to this, detailed studies in PANI doped by CSA have been reported [6]. The above investigations indicate that the localization–interaction model is appropriate to PANI systems near the M–I transition. However, new features like positive magnetoconductance (MC) in PANI-AMPSA has revived the interest in the transport properties of doped PANI. Usually, in less metallic conducting polymers like polypyrrole (PPy) [7],

polythiophenes (PT) [8], and PANI [9], etc, hardly any positive MC is observed, unlike in more metallic conducting polymers like polyacetylene (PA) [10] and poly(phenylene vinylene) (PPV) [11]. Furthermore, Tzamalis *et al* [5] have investigated only the transverse MC in PANI-AMPSA, hence it is of considerable importance to study how the MC varies in both the transverse and longitudinal directions. Typically, in unoriented conducting polymers like PANI, no angular dependence of MC is observed, since the chains are isotropically distributed in the system. However, this study finds a sign variation in the transverse and longitudinal MC, as in oriented metallic conducting polymers like PA [10] and PPV [11], which is quite surprising in the case of the unoriented and less metallic PANI-AMPSA system. Also, a comparison of conductivity and MC among various sulfonic acid doped PANI systems is still lacking in earlier studies.

The subtle variations in crystallinity and morphology are governed by molecular recognition interactions, and that in turn are influenced by the processing conditions. For example, Xia *et al* [12] demonstrated the uncoiling and extension of coiled PANI chains by exposing them to the vapour of polar solvents like *m*-cresol, and consequently some of the localized polarons are delocalized. Further Ikkala *et al* [13] have pointed out that molecular recognition plays a major role in dopant–solvent–polymer chain interactions and nanoscopic scale structural order in the system. Usually, the combination of the dopant counterion and solvent determines the morphology in which the chains can be either extended or coiled. The chain extension improves crystallinity and delocalization of charge carriers, whereas the coiling of chains makes the system more amorphous and granular, resulting in the localization of carriers.

In the present work, PANI has been doped by three commonly used dopants (CSA, DBSA and AMPSA). The behaviour of low temperature conductivity and MR explores the correlation between morphology and nanoscopic transport parameters. The positive MR in PANI-DBSA is significantly larger with respect to that in PANI-CSA, whereas the MC in PANI-AMPSA showed different sign in transverse and longitudinal magnetic field. The sign is positive (negative) for transverse (longitudinal) MC. This indicates that the weak localization contribution to MC is significantly larger, and the hopping contribution is much less in the case of PANI-AMPSA, with respect to other doped PANI systems. Hence the nature of the counterion plays a crucial role in the morphology and charge transport.

2. Experimental procedures

PANI powder was prepared through an oxidative route at $-40\,^{\circ}$C as described by Adams *et al* [18]. Cao *et al* [19] have discovered that doped PANI can be made soluble and easily processible by doping with functional-sulfonic acids, in which the interaction of surfactant-counterion and solvent plays a crucial role in the morphology of the system. The solvents used for casting the films with dopants AMPSA, CSA and DBSA are dichloroacetic acid, *m*-cresol and xylene, respectively. Though optimally processed PANI-CSA films usually have conductivity around 300 S cm^{-1}, the samples in the present study were slightly more disordered so that its conductivity matches that of PANI-AMPSA and PANI-DBSA ($\sim$50 S cm^{-1}). Hence a one to one comparison among these different systems can be made. Free-standing films having thickness 50–70 μm were prepared by drop-casting and subsequent peeling from the silicon substrate. Following the four-in-line geometry, copper wires were attached by conductive carbon adhesive for the measurement of sample resistance. For MR measurements, the samples were placed in a superconducting Janis cryostat (field up to 8 T and temperature down to 1.6 K). The measurements were carried out with a Keithley 220 current source and Keithley 2000 multimeter. The power dissipation in the sample was below 1 μW at low temperatures. The

temperature was measured with calibrated platinum (300–50 K) and carbon glass (1.4–50 K) sensors. A few samples in each system were measured to check the reproducibility of results. The free-standing films were preserved in evacuated desiccators for a period of one to two years. The transport studies on several samples did not show any significant variations over a period of one year.

3. Results and discussion

The room temperature conductivity of AMPSA, CSA and dodecylbenzene sulfonic acid (DBSA) doped PANI is in the range 50–300 S cm^{-1}, depending on the processing conditions. In high quality samples, a positive temperature coefficient of resistivity (TCR) is observed down to 100 K [9], as in typical metals. For example, the PANI-CSA system shows large finite conductivity as $T \rightarrow 0$ [1], metallic reflectance in the infrared [14], temperature-independent Pauli susceptibility down to 20 K [15], linear increase of thermopower with temperature [9], etc. Prior to the surfactant counterion-induced processing procedure, the usual protonic acid (for example HCl, H_2SO_4, etc) doped PANI yielded conductivity of only a few tens of S cm^{-1}, with a strong temperature dependence [16]; as a result hardly any intrinsic metallic behaviour was observed, since the extent of disorder was relatively large, whereas the charge transport property measurements in several functional-sulfonic acid doped PANI have consistently shown intrinsic metallic features [3]. Systems like PANI-CSA have shown a positive TCR at $T > 150$ K, whereas several others like PANI-DBSA hardly show any positive TCR [6]. Surprisingly, the less conducting PANI-AMPSA system [$\sigma(300\ \mathrm{K}) \sim 50$–$100$ S cm^{-1}] has a pronounced positive TCR down to 100 K, whereas in better conducting PANI-CSA samples [$\sigma(300\ \mathrm{K}) \sim 200$–$500$ S cm^{-1}] the positive TCR was observed only down to 150 K [3]. The room temperature conductivities of PANI-AMPSA, PANI-CSA and PANI-DBSA samples in this work are nearly identical [$\sigma(300\ \mathrm{K}) \sim 50$–$80$ S cm^{-1}], so that their transport properties can be compared. Although it is well known that magnetoresistance (MR) is quite appropriate to investigate the effects of disorder and morphology in nanoscopic scale, however, there has not been any detailed investigation of MR as the morphology of PANI is altered by various functional-sulfonic acids.

The temperature dependence of conductivity of doped PANI samples is shown in figure 1. PANI-AMPSA shows a weak metallic behaviour (positive TCR) down to 150 K, and a weak negative TCR below 50 K; a similar behaviour occurs in PANI-CSA too (figure 1(a)). The conductivity is weakly temperature dependent in the case of PANI-DBSA for $T > 50$ K, and it decreases substantially below 50 K (figure 1(b)), as in insulating systems with variable range hopping (VRH) transport. The logarithmic derivative of conductivity, $W = \mathrm{d}\ln\sigma/\mathrm{d}\ln T$, is plotted in the inset of figure 1. This indicates that PANI-CSA and PANI-AMPSA are at the critical regime of the M–I transition, as evident from the nearly temperature-independent activation energy; and the negative temperature coefficient of W for PANI-DBSA confirms its insulating nature. The values of resistivity ratio, ρ_r [$\rho_r = \rho(1.6\ \mathrm{K})/\rho(300\ \mathrm{K})$], for PANI-AMPSA, PANI-CSA and PANI-DBSA are 2.2, 3.2 and 173, respectively. Hence, PANI-AMPSA has one of weakest temperature dependences of conductivity with respect to other doped conducting polymers, though its $\sigma(300\ \mathrm{K}) \sim 50$–$100$ S cm^{-1}.

The low temperature ($T < 4.5$ K) conductivity in the presence of magnetic field (2 and 6 T for PANI-AMPSA and PANI-CSA, 2 and 8 T for PANI-DBSA) for doped PANI samples is shown in figure 2. The conductivity values for AMPSA, CSA and DBSA doped samples, at 1.6 K, are 25, 17 and 0.2 S cm^{-1}, respectively, indicating that AMPSA and CSA doped PANI can have a finite conductivity as $T \rightarrow 0$ K. However, a field of 6 T reduces the conductivity of PANI-CSA, and in PANI-AMPSA it increases slightly, as shown in figure 2.

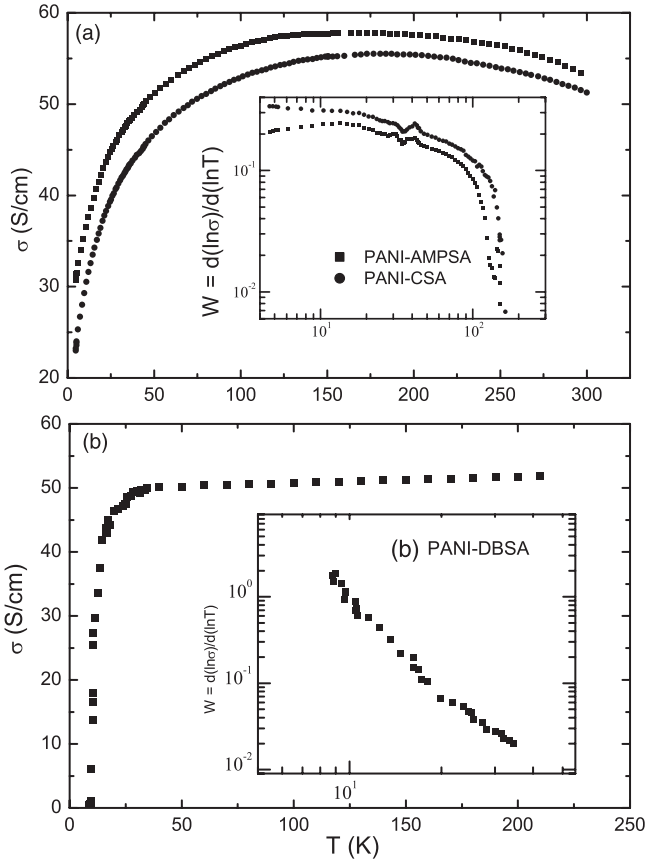

Figure 1. Conductivity versus temperature for (a) AMPSA, CSA and (b) DBSA doped PANI. The inset shows a W versus T plot.

Hence, field increases the low temperature conductivity in PANI-AMPSA, and in the other two it decreases. This strongly suggests that PANI-AMPSA is more metallic with respect to the other two systems, as inferred from the W versus T plot too. These results indicate that the theoretical approach based on localization–interaction models for disordered metallic systems is appropriate for field-dependent low temperature conductivity data analysis.

In the metallic regime, the conduction mechanism at low temperatures ($T < T_{\mathrm{corr}}$) is due to quantum diffusion of quasi-particles, and the conductivity at finite temperatures could be expressed as [20, 21]

$$\sigma(T) = \sigma(0) + mT^{1/2} + BT^{p/2} \tag{1a}$$

$$m = \alpha[(4/3) - (3/2)\gamma F_\sigma] \tag{1b}$$

$$\alpha = (e^2/\hbar)(1.3/4\pi^2)(k_{\mathrm{B}}/2\hbar D)^{1/2} \tag{1c}$$

where $\sigma(0) \sim 0.1e^2/\hbar L_{\mathrm{corr}}$ (L_{corr} being the correlation length), and γF_σ is the interaction term ($\gamma F_\sigma > 0$), where the value of γ depends on the band structure and F_σ is the Hartree factor, D is the diffusion coefficient. The second term in equation (1a) is the lowest order correction to the conductivity arising from electron–electron interaction (EEI) and the third term is the finite temperature localization correction in the less disordered limit. The temperature dependence of the localization correction is determined by the temperature dependence of the inelastic scattering rate $\tau_{\mathrm{in}}^{-1} \propto T^p$ (τ_{in} being the inelastic scattering time) of the dominant dephasing mechanism. For electron–phonon scattering, $p = 2.5$–3; for inelastic electron–

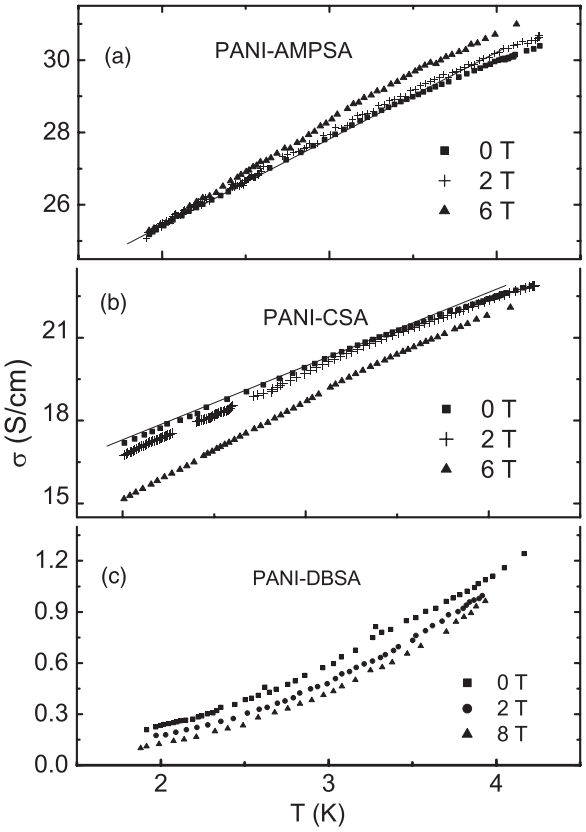

Figure 2. Conductivity versus temperature ($T < 4$ K) at various magnetic fields for (a) PANI-AMPSA, (b) PANI-CSA and (c) PANI-DBSA. The solid lines in (a) and (b) are the fits to equation (1*a*).

electron scattering, $p = 2$ and 1.5 in the clean and dirty limits, respectively. The coefficient m of the EEI term in equation (1*a*) is related to the diffusion coefficient (D) through the relation equation (1*c*). The prefactor m in the interaction term also depends on the magnetic field. When the field exceeds the limit for Zeeman splitting ($g\mu_B H > k_B T$, where g is the gyromagnetic ratio of electron and μ_B is Bohr magneton), equation (1*a*) modifies to [20, 21]

$$\sigma(H, T) = \sigma(H, 0) + m_H T^{1/2} \tag{2a}$$

$$m_H = \alpha[(4/3) - (\gamma F_\sigma/2)]. \tag{2b}$$

The low temperature conductivity data are fitted to equations (1*a*) and (2*a*) for PANI-AMPSA and PANI-CSA, as shown in figures 2(a) and (b). From these fits, the value of D can be estimated, as shown in table 1. More detailed analysis of these parameters is given later.

Since these doped PANI samples are at the critical and insulating regimes it is appropriate to check how well the low temperature data fit to the hopping transport model. Mott's VRH fit to the data is shown in figure 3. The parameters that characterize VRH transport are T_0, localization length (L_c), the mean hopping length (R_{hop}) and mean hopping energy (Δ_{hop}) of the charge carriers. For samples in the insulating regime, the low temperature resistivity follows the exponential temperature dependence

$$\sigma(T) = \sigma_0 \exp[-(T_0/T)^{1/x}] \tag{3}$$

where $x = 4$ for three-dimensional hopping of non-interacting carriers [22, 23]. The characteristic temperature $T_0 = 18/k_B L_c^3 N(E_F)$ (where L_c and $N(E_F)$ are localization length and the density of states at Fermi energy, respectively) is a measure of how far the system has

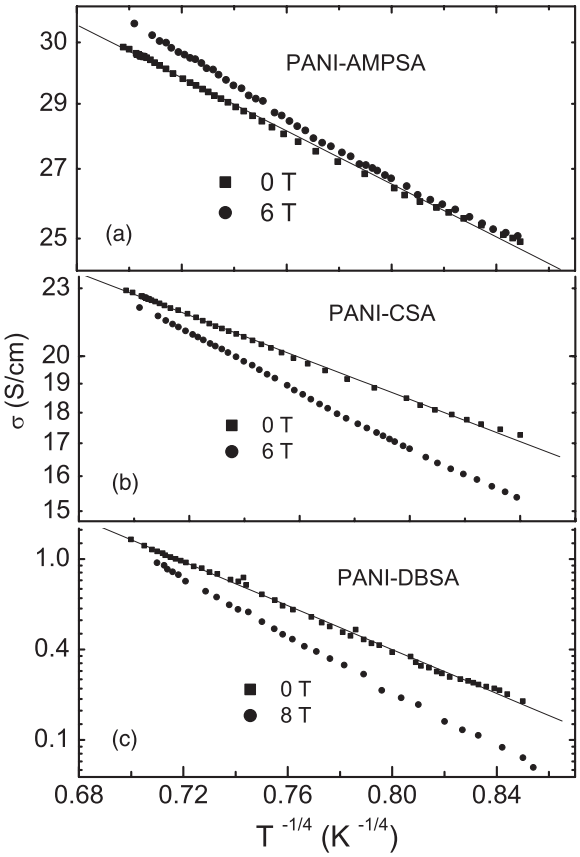

Figure 3. Conductivity versus $T^{-1/4}$ for (a) PANI-AMPSA, (b) PANI-CSA and (c) PANI-DBSA. The solid lines are fits made by equation (3) (at $x = 4$) for the determination of T_0 as listed in table 1.

Table 1. Transport parameters for PANI-AMPSA, PANI-CSA and PANI-DBSA obtained by fitting various models to the data.

Sample	ρ_r [a]	T_0 [b] (K)	L_c [b] (Å)	R_{hop} [c] (Å)	l_{in} [d] (Å)	L_T [e] (Å)	$\Delta\sigma/\sigma$ [f] (%)	Δ_{hop} [c] (eV)	D ($cm^2\ s^{-1}$)
PANI-AMPSA	2.2	3	211	254	132	45	2.5 -8.3[g]	2.4×10^{-4}	7.6×10^{-2}
PANI-CSA	3.2	24	287	184		35	-15	1×10^{-4}	4.4×10^{-2}
PANI-DBSA	173	21 647	128	450			-62	5.6×10^{-4}	

[a] $\rho_r = \rho(1.6\ K)/\rho\ (300\ K)$.
[b] T_0 and L_c are as defined in equations (3) and (7) (Mott's VRH theory) (see figures 3 and 4).
[c] R_{hop} and Δ_{hop} are calculated at $T = 2.8$ K using equations (5) and (6) (Mott's VRH theory).
[d] l_{in} is the inelastic scattering length estimated from the field dependence of MC for PANI-AMPSA at $T = 2.8$ K and equation (8) (WL-EEI model for disordered metallic system) (see figure 7).
[e] $L_T = (\hbar D/k_B T)^{1/2}$, is the interaction length.
[f] Normalized MC at 1.6 K and 6 T (see figures 5 and 6).
[g] Longitudinal MC for PANI-AMPSA.

moved to the insulating side. In VRH transport the charge carriers exhibit thermally activated transport between localized sites, in which the hopping takes place between energetically favourable sites at arbitrary distance. In VRH,

$$\log_{10} W(T) = A - x \log_{10} T \tag{4}$$

where $A = x \log_{10} T_0 + \log_{10} x$. Using equation (4), it is possible to determine both T_0 and x from the data. For Mott's VRH, the mean hopping length (R_{hop}) and mean hopping energy (Δ_{hop}) are estimated from the following expressions [22, 23]:

$$R_{hop} = (3/8) L_c \, (T_0/T)^{1/4} \tag{5}$$

and

$$\Delta_{hop} = (1/4) k_B T \, (T_0/T)^{1/4}. \tag{6}$$

The characteristic Mott temperatures (T_0) for various doped PANIs are determined by fitting equations (3) and (4). Although PANI-AMPSA is just at the metallic side of the critical regime of the M–I transition, the $T^{-1/4}$ fit yields a straight line with a very small value for T_0, $\sim$ 3 K. Hence this fit is not be fully appropriate for PANI-AMPSA, and the hopping contribution to charge transport is quite negligible. Furthermore, the field dependence of conductivity is quite opposite to that typically observed in hopping transport: instead of a decrease of conductivity, it increased in the presence of field. In the case of PANI-CSA, the $T^{-1/4}$ fit yields a straight line with a small value for T_0, $\sim$23 K. The value of T_0 at 6 T is 63 K. If the hopping contribution was rather dominant then the value of T_0 should have increased to much higher values at 6 T field. This suggests that PANI-CSA is barely on the insulating side of the critical regime. So, the fits to the same data by using the localization–interaction model, as shown in figures 2(a) and (b), are much more physically appropriate than the hopping transport model, since the values of T_0 are much below the typical values ($\sim$ a few hundreds of kelvins) observed in insulating systems near the M–I transition. However, from earlier studies it is known that the critical regime in conducting polymers is not that really sharp, as in doped crystalline inorganic semiconductors [1]. Hence approaching the conducting polymer system from either side, by using the localization–interaction model for metallic sides, and the hopping model for insulating sides, looks quite appropriate, since the obtained quantitative numbers (see table 1) for the physical parameters from both analyses are quite reasonable. Moreover, it enriches and completes the analysis.

In both AMPSA and CSA doped PANI, it is really surprising to find that in disordered q-1D system with $\sigma(300\ \mathrm{K}) \sim 50\ \mathrm{S\,cm^{-1}}$, the hopping contribution to low temperature transport is quite negligible. This further suggests that the case of severe disorder-induced localization in one-dimensional (1D) systems is nearly absent in these samples. Moreover, if the crystalline domains are connected via amorphous 1D regions, then quite obviously there is strong localization in these 1D regions, and the associated strong contribution of hopping transport is expected at low temperatures. On the contrary, delocalized transport was observed, especially in the case of PANI-AMPSA, whereas the large value for T_0 (=21 647 K) in PANI-DBSA [$\sigma(300\ \mathrm{K}) \sim 50\ \mathrm{S\,cm^{-1}}$, $\rho_r = 173$] indicates the presence of 1D localization.

To further check how far the hopping transport model is valid in these systems, the magnetic field dependence of Mott's VRH is plotted in figure 4. The typical field dependence is given by [24]

$$\ln[\rho(H)/\rho(0)] = t(L_c/L_H)^4 (T_0/T)^{3/4} \tag{7}$$

where $t = 0.002\,48$ and L_H ($=(\hbar/eH)^{1/2}$) is the magnetic length. From equation (6), by knowing the value of T_0 it is possible to estimate L_c. Although the value of T_0 for PANI-AMPSA is rather small (3 K), the estimated value of L_c gives a reasonable number of 211 Å, whereas for PANI-CSA, with a slightly higher value of T_0(24 K), $L_c = 279$ Å. These values are rather close to the number for L_c obtained in previous works [9]. In the insulating PANI-DBSA sample, with a very large value for T_0 (21 647 K), L_c is much lower (=116 Å). Although the values of T_0 among these samples have a rather wide range, the estimated values for L_c are within reasonable limits, that are usually observed in VRH systems near the M–I transition. We

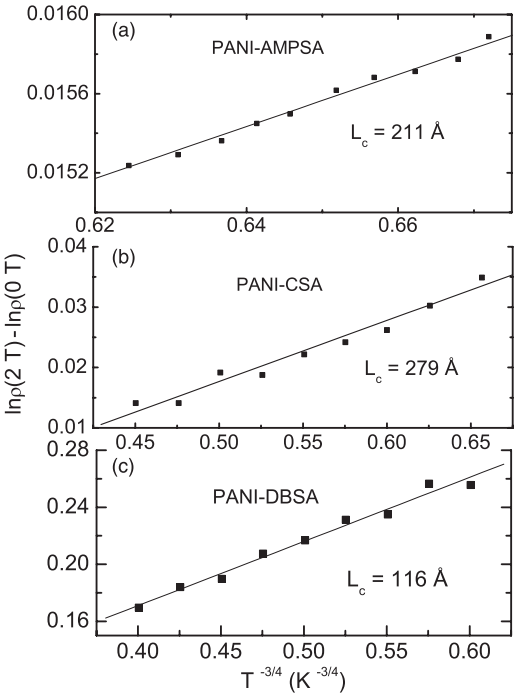

Figure 4. $\ln \rho$ (2 T)–$\ln \rho$ (0 T) versus $T^{-3/4}$ for (a) PANI-AMPSA, (b) PANI-CSA and (c) PANI-DBSA. The straight lines are fits made by equation (7) for the determination of L_c as listed in table 1.

further verified how comparable these values of L_c are with other length scales in the system, for example the mean hopping length (R_{hop}), as shown in table 1. These values are quite comparable. For the insulating PANI-DBSA sample, R_{hop} is quite large (450 Å) with respect to others, as expected. The estimated value for hopping energy (see table 1) is comparable with respect to other VRH systems like Si:As (48 μeV at 2.8 K) [25]. This indicates that the disorder potentials are rather shallow, contrary to that expected in the case of strong disorder in q-1D systems. These estimated parameters show the consistency of data analysis, and the appropriateness of using the models.

The above analysis has given several values for the length scales in both PANI-AMPSA and PANI-CSA systems. Using these quantitative parameters, a back calculation was carried out to check whether it gives realistic numbers for conductivity, $N(E_F)$, etc. $\sigma(0)$ for PANI-AMPSA is nearly 14 S cm^{-1}, as obtained from the fit to data in figure 2(a). The values of D (from equation (1c)) for PANI-AMPSA and PANI-CSA are given in table 1. Using these values the back calculated value of $N(E_F)$ for PANI-AMPSA is 2 states/eV/two rings (by using the equation, $\sigma(0) = e^2 N(E_F) D$), which is in good agreement with reported values for doped PANI [2, 3]. In the case of PANI-CSA, the reported value of $N(E_F) \sim 0.7$ states/eV/two rings [2] is used to back calculate the $\sigma(0)$, and it is nearly 3 S cm^{-1}. The value of $\sigma(0)$, obtained by fitting the PANI-CSA data in figure 2(b) to equation (1a), is nearly 9 S cm^{-1}. Hence the back calculated values of $\sigma(0)$ are rather close. Furthermore, the interaction length $[L_T = \hbar D/(k_B T)^{1/2}]$ for both PANI-AMPSA and PANI-CSA, at 2.8 K, is estimated, and the values are 45 and 35 Å, respectively. While applying the localization–interaction model in any disordered systems, a comparison of L_T and L_c is required, since the criterion $L_T < L_c$ has to be justified. Indeed, the values of L_T are much lower than L_c for both PANI systems. This again verifies the validity of the model, and the consistency in data analysis. Hence this analysis shows that in conducting polymer systems near the M–I transition, approaching the system

from the metallic side via the localization–interaction model and approaching the system from the insulating side via the VRH model can yield quite useful complementary results. Unlike in other systems near the M–I transition, the complicated morphology in conducting polymers can cause the localization-induced M–I transition to be more complex and fuzzy, that in a advantageous way makes it conducive to investigate the M–I transition from either side of the transition.

In general, MC is a useful tool for investigating the interplay of EEI, weak localization (WL) and hopping transport in disordered systems, especially near the M–I transition. Previous studies in conducting polymers like PPy [7], PA [10], PPV [11, 17] have shown that MC data is quite essential to get a quantitative level understanding of nanoscopic scale transport parameters. The total low-field MC ($g\mu_B H \ll k_B T$ for EEI) is given by the following expression [20, 21]:

$$\Delta\Sigma_L(H,T) = (1/12\pi^2)(e/\hbar)^2 G_0 (l_{in})^3 H^2 - 0.041(g\mu_B/k_B)^2 \alpha\gamma F_\sigma T^{-3/2} H^2 \tag{8}$$

where the first and second terms on the right-hand side are due to WL and EEI contributions, respectively; $G_0 = e^2/\hbar$ and l_{in} is the inelastic scattering length. Typically, WL gives rise to positive MC, and EEI results in negative MC. In isotropic 3D systems, the upper bound for corrections due to WL and EEI are approximately +3 and −3%, respectively. However, in disordered q-1D systems like conducting polymers both contributions can vary by a factor of two [20]. At high fields ($g\mu_B H \gg k_B T$), the positive (negative) MC due to WL (EEI) is proportional to $H^{1/2}$. Thus, the total high field MC is given by [20, 21]

$$\Delta\Sigma_L(H,T) = B_{EE} H^{1/2} + B_{WL} H^{1/2} \tag{9a}$$

$$B_{EE} = -0.77(g\mu_B/k_B)^{1/2} \alpha\gamma F_\sigma \tag{9b}$$

$$B_{WL} = (e^2/2\pi^2\hbar)(eH/\hbar)^{1/2} f(x) \tag{9c}$$

where $x = \hbar/(4eHl_{in}^2)$, and $f(x)$ has the asymptotic forms, $f(x) = 0.605$, $x \ll 1$, and $f(x) = x^{-3/2}/48$, $x \gg 1$. The first term on the right-hand side of equation (9*a*) describes the contribution from EEI, and the second term is due to WL, which is nearly 1 S cm^{-1} T$^{-1/2}$ at high field [26].

The MC of doped PANIs is shown in figure 5. PANI-AMPSA shows a positive MC (figure 5(a)), and it is nearly 2.5% at 1.6 K and 6 T in the transverse direction. Similarly Tzamalis *et al* have reported a positive transverse MC in PANI-AMPSA. This is quite consistent with the values expected from the WL contribution. However, at $T < 3$ K, the increase in MC is suppressed by a negative MC contribution, that could be due to both EEI and hopping transport. Since the positive MC has decreased by nearly a factor of two at $T < 3$ K (from 4% at 2.8 K to 2% at 1.6 K), the hopping contribution to this decrease should be considerably more with respect to EEI. The MC for PANI-CSA is shown in figure 5(b). The negative MC in this system clearly indicates that the WL contribution is quite negligible, and the EEI and hopping contributions are rather dominant. Especially at $T < 3$ K, the hopping contribution should be considerably more with respect to EEI, since the negative MC (∼−15% at 1.6 K and 6 T) is much larger than that expected from the EEI contribution (∼−3% at 1.6 K and 6 T). Although ρ_r for PANI-AMPSA (2.2) and PANI-CSA (3.2) are rather close, and both systems are at the critical regime of M–I transition, the behaviour of MC is drastically different, as explained below. The large positive MR (∼200% at 1.6 K at 8 T) for PANI-DBSA is shown in figure 5(c). This is quite expected since ρ_r for PANI-DBSA is 173, and the system is in VRH transport (as in figure 3(c)). In both PANI-CSA and PANI-DBSA there is hardly any variation among the transverse and longitudinal MR.

Since PANI-AMPSA has shown a positive MC in the transverse direction, it is really curious to find out how the MC in the longitudinal direction behaves. Moreover, Tzamalis *et al* [5]

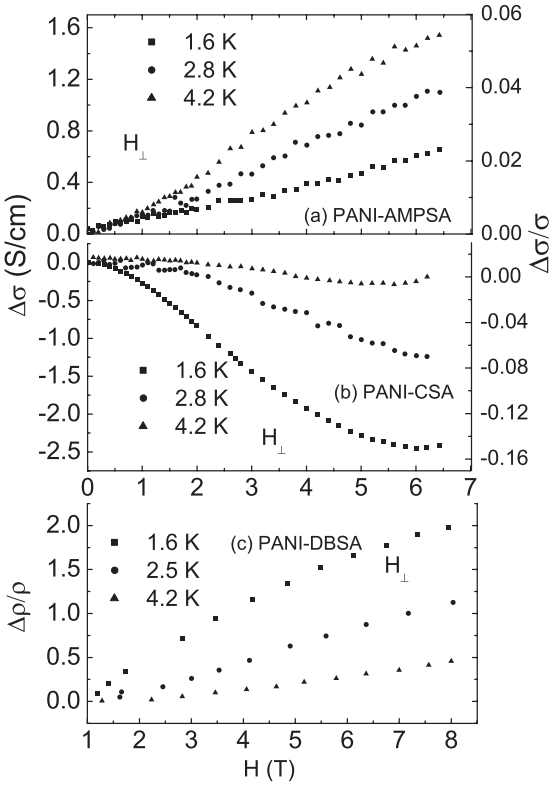

Figure 5. Transverse magnetoconductance (MC) versus H at various temperature for (a) PANI-AMPSA and (b) PANI-CSA. Normalized transverse MC ($\Delta\sigma/\sigma$) is shown at the right-hand axis. Normalized transverse magnetoresistance ($\Delta\rho/\rho$) versus H at various temperatures for PANI-DBSA is shown in (c).

have not reported any longitudinal MC data. This has motivated us to carry out the longitudinal MC, as shown in figure 6. It is really surprising that the sign of MC is negative at all temperatures and fields. Such an anisotropic MC is hard to expect in a barely metallic unoriented conductive polymer system like PANI-AMPSA. Of course, earlier studies in highly oriented metallic PA [10] and PPV [11] have shown anisotropic MC. The negative MC increases substantially at $T < 3$ K. These data suggest that there is hardly any WL contribution in longitudinal MC, unlike in the case of transverse MC. The negative longitudinal MC is largely due to the contributions from EEI and hopping transport, in which the latter dominates at $T < 3$ K.

Although the room temperature conductivity of all three doped PANI systems is nearly the same ($\sim$50 S cm^{-1}), the behaviour in MC is substantially different. This indicates that the dopant counterion plays a significant role in the local molecular scale structure, and this influences the nanoscopic level transport properties. First, the anisotropic MC in PANI-AMPSA suggests the formation of molecular scale quasi-two-dimensional (q-2D) structures, which is not possible in other doped PANI samples. In the AMPSA counterion, the acrylamido group (containing both C=O group and π-electron group (CH_2=CH) at the end) is quite different from counterions like CSA and DBSA. The ability of the C=O bond to make hydrogen bonding with the N–H group is well known, especially when they are in close proximity [27]. Such a hydrogen bonding between the C=O group in AMPSA and the N–H group in the PANI chain can bring the CH_2=CH end group in close proximity to the chains, thus the steric hindrance is quite minimal for these π-electrons to make a π–π interaction with the segments in the PANI chain. The more ordered regions have larger intermolecular π-electron

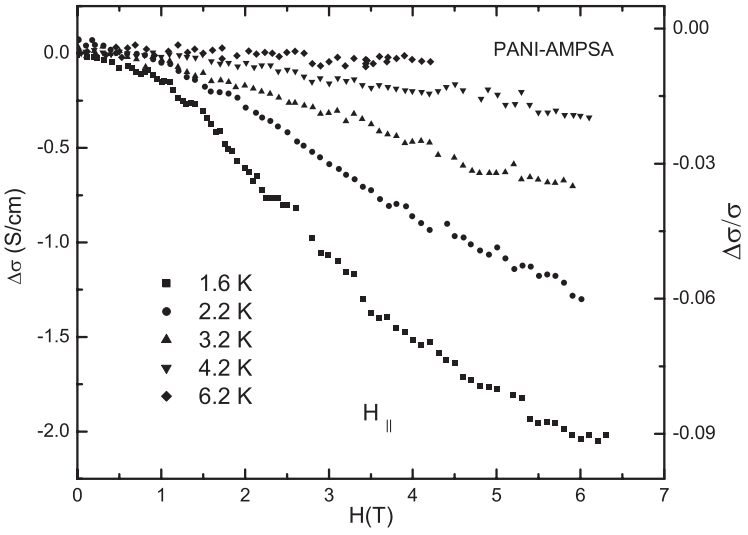

Figure 6. Longitudinal magnetoconductance (MC) versus H for PANI-AMPSA at various temperatures.

interaction than the less ordered regions. Hence, in the case of AMPSA doped PANI, the acrylamido group can enhance the molecular scale ordering of PANI chains via hydrogen bonding and π–π interaction. Moreover, this type of intermolecular π–π interactions among various segments in PANI chain can form local q-2D electronic structures in which the charge carriers are fairly delocalized. This special structural feature in PANI-AMPSA could explain the anisotropic MC due to the presence of delocalized carriers in local self-assembled q-2D structures, whereas in CSA and DBSA doped PANI, such interactions are quite weak; as a result the delocalized electronic states in partially ordered domains are rather close to q-1D structures. Furthermore, the ESR spectra of PANI-AMPSA is quite different from other doped PANI, and it shows certain features due to the local q-2D ordering [28]. Although CSA is a more effective counterion, with respect to DBSA, in bringing molecular-scale ordering of PANI segments [13], in both cases even slight variations in the extent of disorder in q-1D structures can influence the coherent transport dramatically. The large negative MC in both CSA and DBSA doped PANI shows the dominant contribution of hopping transport, unlike in the case of PANI-AMPSA, as shown in figures 5 and 6. The highly insulating behaviour of PANI-DBSA indicates that there is hardly any ordered region in this system, in comparison to the other two.

Furthermore, in the case of extended chains in q-2D regions, the π–π interaction of the benzene rings among adjacent PANI chains can help to reduce the torsional angle between them; as a result, the interchain transfer integral ($t_\perp$) increases [29, 30]. In q-1D systems like conducting polymers, it is known that $t_\perp$ should be sufficiently large enough to have the wavefunctions extend over to neighbouring chains to facilitate coherent interchain transport [29]. Moreover, in extended chain conformation it is possible to achieve $t_\perp \geqslant U$ (where U is the Coulomb correlation energy), which favours the formation of the delocalized metallic state in conducting polymers. Recent optical studies have shown that when $t_\perp \geqslant$ 0.15 eV, the confined polarons get substantially delocalized over adjacent chains [31]. In this scenario, both interaction and disorder-induced localization play crucial roles in the M–I transition of conducting polymers. Even slight variations in the π-electron overlap of adjacent PANI chains can have a significant impact on the localization–delocalization transition. This subtle correlation between structural and electronic properties can be observed in the charge transport properties of surfactant-counterion doped PANI.

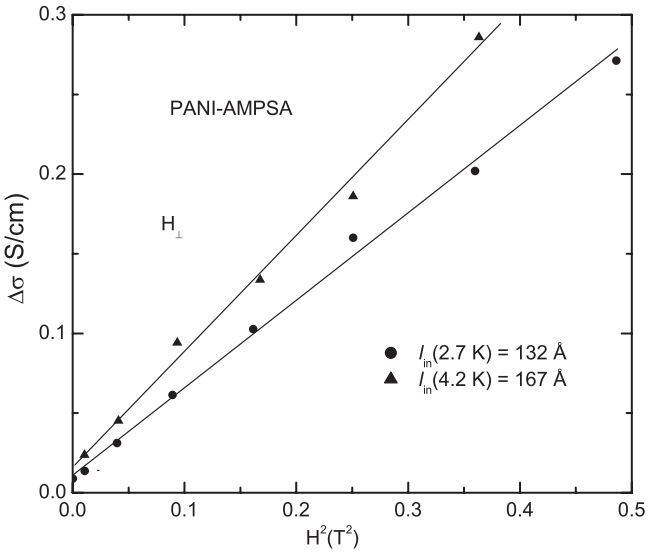

Figure 7. Transverse magnetoconductance ($\Delta\sigma$) versus H^2 at low field ($g\mu_B H \ll k_B T$) for PANI-AMPSA. The solid lines are the fits made by equation (8) at temperature $T = 2.8$ and 4.2 K for the estimation of l_{in} as listed in table 1.

The anisotropic MC, especially at $T < 3$ K, for PANI-AMPSA is further scrutinized. The effect of magnetic field on the negative contribution to MC is much more dominant in the longitudinal direction. The data in figures 5(a) and 6 show that the increase in negative longitudinal MC (from -2 at 4.2 K and 6 T to -9% at 1.6 K and 6 T) is much larger with respect to the slight lowering of positive transverse MC (from +4 at 4.2 K and 6 T to +2% at 1.6 K and 6 T). This difference cannot be accounted for solely by the EEI contribution, since the variation is too large. Apart from the WL-EEI contribution, this anisotropy is due to different degrees of the stretch to the wavefunctions of electronic states in the longitudinal ($\lambda_\parallel$) and transverse ($\lambda_\perp$) directions in the presence of magnetic field, especially in the case of two-dimensional (2D) structures. This additional hopping contribution to MC, at $T < 3$ K, is due to the anisotropy in carrier hopping in the transverse and longitudinal directions [24], that is given by $\sigma_\parallel/\sigma_\perp = (\lambda_\perp/\lambda_\parallel)^2$. In the case of PANI-AMPSA $\lambda_\perp < \lambda_\parallel$, which explains why the contribution of negative MC due to hopping is larger in longitudinal than in transverse MC.

The total low-field MC, as given by equation (8), is plotted as $\Delta\sigma$ versus H^2, as in figure 7. The low-field contributions due to WL and EEI are fitted to equation (8). The slope of the straight line fit yields the value of l_{in} (132 and 167 Å at 2.8 and 4.2 K, respectively). The obtained values are quite appropriate with respect to other length scales like L_c and R_{hop}, as shown in table 1. The values of l_{in}, L_c and R_{hop} are fairly close, since the system is near the critical regime of the M–I transition. This further shows that the WL + EEI model is appropriate in PANI-AMPSA, especially at low fields. Although Tzamalis *et al* have observed a deviation from the WL + EEI model at fields above 8 T, this could be attributed to other types of field-induced delocalization mechanisms, especially at high fields [32]. More detailed anisotropic MC studies at high fields are required to clarify this further.

An important consequence of magnetotransport dominated by EEI is the universal scaling of MC. According to this scaling theory, the general form of MC at low fields ($g\mu_B H \ll k_B T$) due to EEI is given by the following expression [11]:

$$\Delta\sigma/T^{1/2} = -0.041\alpha\gamma F_\sigma (g\mu_B/k_B)^2 (H/T)^2. \tag{10}$$

If the MC is entirely dominated by EEI, a plot of $\Delta\sigma/T^{1/2}$ versus H/T (scaling plot) for any value for H and T should collapse to equation (10) in a single line, as shown by Bogdanovich *et al* [33]. Similar scaling of MC due to EEI has been observed in

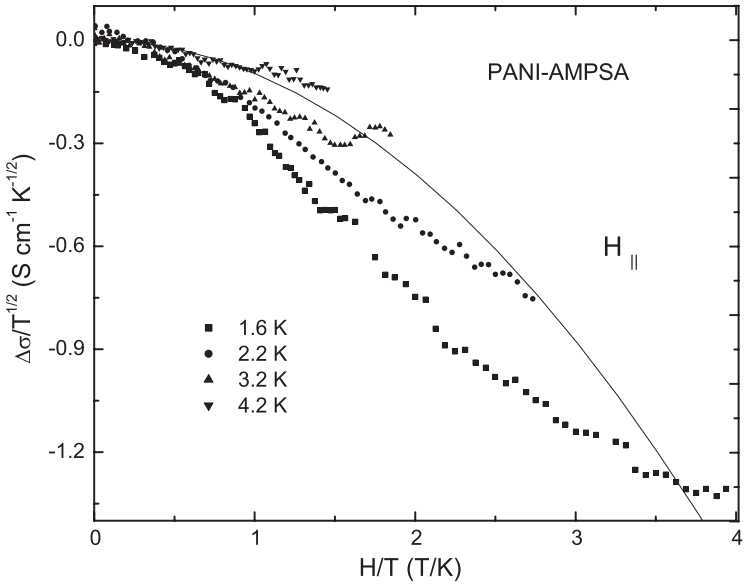

Figure 8. Scaling plot: scaled longitudinal MC ($\Delta\sigma/T^{1/2}$) versus (H/T) for PANI-AMPSA, at various temperatures. The solid curve is the theoretical curve, $\Delta\sigma/T^{1/2} = -0.098(H/T)^2$ as deduced from equation (10).

metallic PPV [11] and poly(3,4-ethylene dioxythiophene) [34]. The scaling plot of the longitudinal MC data for PANI-AMPSA is shown in figure 8. The estimated theoretical curve [$\Delta\sigma/T^{1/2} = -0.098(H/T)^2$ for $\alpha = 7.4$ S cm^{-1} K$^{-1/2}$, $\gamma F_\sigma = 0.18$] from equation (10) is also plotted in the same figure, which is purely due to the EEI contribution. The data up to $H/T \sim 1$, at all four temperatures, collapse to the theoretical line, as shown in figure 8. Hence, at low-field, EEI is dominating the longitudinal MC. However, at $H/T > 1$ there is substantial deviation from the theoretical line, at all temperatures. This additional contribution to the negative longitudinal MC is due to the hopping transport, as observed earlier in figure 6. Hence this scaling plot further confirms the role of hopping transport. A similar scaling plot for MC has been attempted for transverse MC in PANI-AMPSA, in which there is hardly any collapse to the theoretical line for any values of H/T, indicating that the scaling due to EEI is nearly absent.

4. Conclusions

Although the room temperature conductivity ($\sim$50 S cm^{-1}) of PANI doped AMPSA, CSA and DBSA are nearly identical, the temperature dependence of conductivity and magnetotransport are rather different. The values of ρ_r for PANI doped AMPSA, CSA and DBSA are 2.2, 3.2 and 173, respectively. The W versus T plot shows that PANI-AMPSA and PANI-CSA are barely on the metallic side of the critical regime (positive TCR at $T > 150$ K), and PANI-DBSA in VRH transport regime. The transverse (longitudinal) MC is positive (negative) in PANI-AMPSA. This anisotropic MC is consistent with WL (positive MC) and EEI (negative MC) models, with an additional weak hopping transport contribution at $T < 3$ K. This anisotropic MC suggests the presence of local molecular-scale q-2D ordered regions in PANI-AMPSA. The negative MC in PANI-CSA and PANI-DBSA, at 1.6 K and 6 T field, is 15 and 62%, respectively. The

values for l_{in} (at 2.8 K) and L_c for PANI-AMPSA are 132 and 211 Å, respectively. The data analysis by the WL + EEI model (on the metallic side) and the VRH model (on the insulating side) yields consistent values for L_T, l_{in}, L_c and R_{hop}. The longitudinal MC of PANI-AMPSA scales up to $H/T \sim 1$, and the deviation for $H/T > 1$ is due to the contribution from hopping transport.

Hence PANI doped with surfactant counterions like CSA, DBSA and AMPSA shows a wide range of properties, in which interactions of the PANI chain and counterions play a significant role in the local order of the system that determines the transport properties. These results show that specially tailored dopant counterions can induce self-assembled ordered regions in the systems with improved physical properties. The low temperature magnetotransport studies are highly useful in finding out these structure–transport relations in conducting polymers, as demonstrated in the case of doped PANI in this work.

References

[1] Menon R, Yoon C O, Moses D and Heeger A J 1998 *Handbook of Conducting Polymers* ed T A Skotheim *et al* (New York: Dekker) p 27
Menon R 1997 *Handbook of Organic Conductive Molecules and Polymers* ed H S Nalwa (New York: Wiley) p 47
[2] Kohlman R S and Epstein A J 1998 *Handbook of Conducting Polymers* ed T A Skotheim *et al* (New York: Dekker) p 85
[3] Adams P N, Devasagayam P, Pomfret S J, Abell L and Monkman A P 1995 *J. Chem. Phys.* **10** 8293
[4] Menon R, Cao Y, Moses D and Heeger A J 1993 *Phys. Rev.* B **47** 1758
[5] Tzamalis G, Zaidi N A and Monkman A P 2003 *Phys. Rev.* B **68** 245106
[6] Pron A, Rannou P, Gawlicka A, Berner D, Nechtschein M, Bajer I K and Djurado D 1999 *Synth. Met.* **101** 729
[7] Yoon C O, Menon R, Moses D and Heeger A J 1994 *Phys. Rev.* B **49** 10851
[8] Masubuchi S, Fukuhara T and Kazama S 1997 *Synth. Met.* **84** 601
[9] Menon R, Yoon C O, Moses D, Heeger A J and Cao Y 1993 *Phys. Rev.* B **48** 17685
[10] Menon R, Vakiparta K, Cao Y and Moses D 1994 *Phys. Rev.* B **49** 16162
[11] Ahlskog M, Menon R and Heeger A J 1996 *Phys. Rev.* B **53** 15529
[12] Xia Y, MacDiarmid A G and Epstein A J 1994 *Macromolecules* **27** 7212
[13] Ikkala O T, Pietila L-O, Ahjopalo L, Osterholm H and Passiniemi P J 1995 *J. Chem. Phys.* **103** 9855
[14] Lee K, Heeger A J and Cao Y 1995 *Synth. Met.* **72** 25
[15] Sariciftci N S, Heeger A J and Cao Y 1994 *Phys. Rev.* B **49** 5988
[16] Wang Z H, Scherr E M, MacDiarmid A G and Epstein A J 1992 *Phys. Rev.* B **45** 4190
[17] Ahlskog M, Menon R and Heeger A J 1997 *Phys. Rev.* B **55** 6777
[18] Adams P N and Monkman A P 1997 *Synth. Met.* **87** 165
[19] Cao Y, Smith P and Heeger A J 1992 *Synth. Met.* **48** 91
[20] Lee P A and Ramakrishnan T V 1985 *Rev. Mod. Phys.* **57** 287
[21] Dai P, Zhang Y and Sarachick M P 1992 *Phys. Rev.* B **45** 3984
[22] Mott N F and Davis E A 1979 *Electronic Processes in Noncrystalline Materials* (Oxford: Oxford University Press)
[23] Mott N F 1990 *Metal Insulator Transition* 2nd edn (London: Taylor and Francis)
[24] Shklovskii B I and Efros A L 1979 *Electronic Properties of Doped Semiconductors* (Berlin: Springer)
[25] Shafarman W N and Castner T G 1986 *Phys. Rev.* B **33** 3570
[26] Ahlskog M and Menon R 1998 *J. Phys.: Condens. Matter* **10** 7171
[27] Kuhnert N and Gresley A Le 2003 *Chem. Commun.* 2426 and references therein
[28] Sitaram V *et al* 2005 at press
[29] Hirsch M J 1987 *Comments Condens. Mater. Phys.* **13** 249
[30] Romijn I G, Hupkes H J, Martins H C F, Brom H B, Mukherjee A K and Menon R 2003 *Phys. Rev. Lett.* **90** 176602
[31] Wohlgenannt M, Jiang X M and Vardeny Z V 2004 *Phys. Rev.* B **69** 241204(R)
[32] Prigodin V N and Roth S 1993 *Synth. Met.* **53** 237
[33] Bogdanovich S, Dai P and Sarachick M P 1995 *Phys. Rev. Lett.* **74** 2543
[34] Aleshin A, Kiebooms R, Menon R, Wudl F and Heeger A J 1997 *Phys. Rev.* B **56** 3659